THERMAL RADIATION MODELLING OF DC SMELTING FURNACE FREEBOARDS

Q. Reynolds
Mintek, Private Bag X3015, Randburg, 2125, South Africa
E-mail for correspondence: quinnr@mintek.co.za

Abstract

The problem of radiation heat transfer in a system of large numbers of surface elements was considered. A numerical-mathematical model detailing the radiative exchange between surfaces in a generalised multiple-surface shape model was constructed, developed, and tested to a satisfactory degree of complexity, at which point it was incorporated into a general-purpose computer program.

Predictions by the model were compared to selected results from pilot-scale DC arc furnace tests run at Mintek, to evaluate the significance of radiation heat transfer to the overall energy loss from the freeboard regions of such furnaces.

Finally, the model was used to examine a range of process and design variables, and scale-up issues. Several interesting aspects and phenomena come out of the exhaustive modelling work, to hopefully aid the designer of DC arc furnace freeboards in the future on both the pilot and full industrial scale.

Keywords

Modelling, Pyrometallurgy

INTRODUCTION

Existing work in the field of heat transfer modelling of smelting furnace behaviour has been fairly widespread, treating a great range of processes and furnace designs.

Much work has been done in the field of computational fluid dynamic (CFD) modelling, with particular reference to dealing with electromagnetically driven high-temperature flows in the plasma arc region of the furnace, and flow in the molten bath below it, as in Szekely et al (1983) and others. These models attempt to predict thermal and electrical behaviour of the electric arc column and its surroundings by solving the coupled partial differential equations of heat and momentum transfer, and electromagnetics numerically. However, the extent to which radiation energy transfer is dealt with is generally limited to approximate calculations of direct radiation from the arc impinging on the freeboard surfaces, as in Ushio et al (1981), and while it is often noted that the bath surface does transmit substantial amounts of thermal radiation to the other freeboard surfaces, this factor is usually grossly neglected or over-simplified. At best, the bath surface radiation is taken into account by solving for a small system of large, thermally uniform surfaces as with the approach taken by Holt & Bakken (1993).

Bowman (1994) documents experimental measurements of the behaviour of such furnaces at full and substantial pilot-plant scale, and Deneys & Robertson (1998) do the same in the laboratory, although again radiation is neglected to some degree, with only net energy loss numbers measured if at all. It is left to the researcher to infer a mechanistic explanation for the contribution of the various components to the total energy losses.

The development of a detailed model of the thermal radiation transfer from the molten bath surface to the upper sidewall and roof areas of the DC plasma-arc smelting furnace is thus desirable.

DEVELOPMENT OF THE MULTIPLE-REGION RADIATIVE EXCHANGE MODEL

In the analytical approach to surface radiation problems, one derives an energy balance on each of the surfaces participating in the energy exchange in turn, thereby generating a set of equations (two for

each surface in the system for grey bodies) representing a total energy balance. These energy balance equations are seen to contain terms pertaining to direct emission of thermal radiation from the surface, incident radiation either directly from or reflected from other surfaces, and external sources or sinks. This approach has been developed and presented by Hottel & Sarofim (1967) for all surfaces opaque and radiating as grey bodies, where a single value of the average hemispherical surface emissivity, ε may be assigned to each surface's material across the entire wavelength spectrum.

Consider a partial enclosure of N discrete surfaces, all of which are absorbing, emitting, and reflecting radiant energy between each other. Assumptions for the case of the grey body model are:

- The surfaces are grey and opaque (an acceptable approximation in the case of the solids and liquids dealt with in smelting furnaces), that is, that a fraction ε of any radiation incident on the surface is absorbed and the rest (1-ε) reflected, with ε=α independent of the wavelength of the irradiation.
- Reflection from the surfaces is diffuse, meaning that a beam's direction once it leaves the surface is independent of its direction of incidence upon the surface. This is generally the case for unpolished, rough surfaces.

In the enclosure, an energy balance over a single surface is obtainable:

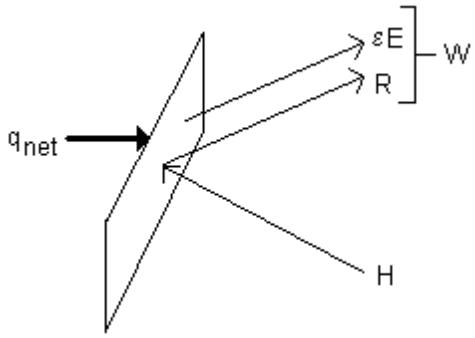

Figure 1 *- Energy balance over single grey surface*

Incident radiation flux H_k from other parts of the system impinges on surface k. A portion of this flux is reflected (R_k), and this radiative component is complemented by direct emission from the surface $\varepsilon_k E_k$. Together, these two components give the total radiative flux emission from the surface, W_k. The difference between H and W gives the net energy input or output to the surface by means other than radiation, $q_{net,k}$.

The energy balance is expressed as follows:

$$W = \varepsilon E + R$$
$$R = (1-\alpha)H = (1-\varepsilon)H \qquad \textbf{(1)}$$
$$W = \varepsilon E + (1-\varepsilon)H$$

and also:

$$q_{net} = W - H = W - \frac{R}{1-\varepsilon} = W - \frac{W-\varepsilon E}{1-\varepsilon} = \frac{\varepsilon}{1-\varepsilon}\left(E - W\right) \qquad \textbf{(2)}$$

Now an expression for the incident radiation flux H is required. Consider that there are N surfaces in the system, each emitting a flux W_i with i = 1...N. For a given i, a certain fraction of the flux emitted from surface i is seen by surface k. The fraction is termed the view factor and represents the geometric attenuation of radiative exchange occurring between a pair of surfaces due to their relative orientation and shape. The definition of the view factor is most often represented as a double integral over the two participating surfaces:

$$F_{ik} = \frac{1}{A_i}\iint_{A_i,A_k} \frac{\cos\theta_i \cos\theta_k dA_i dA_k}{\pi\left|\mathbf{r_{ik}}\right|^2} \qquad \textbf{(3)}$$

Here, $\mathbf{r_{ik}}$ is the displacement vector between points on surfaces i and k, and θ_i and $\theta_k$are the angles that $\mathbf{r_{ik}}$ makes with the normal vectors on i and k.

Given this definition it is seen that:

$$A_k H_k = \sum_{i=1}^{N} A_i F_{ik} W_i \tag{4}$$

since all radiation incident upon surface k originates from other surfaces in the system. Which by substitution from above is seen to yield:

$$\frac{W_k - \varepsilon_k E_k}{1-\varepsilon_k} = H_k = \sum_{i=1}^{N} \frac{A_i}{A_k} F_{ik} W_i = \sum_{i=1}^{N} F_{ki} W_i \tag{5}$$

The system of equations to be solved thus becomes:

$$\begin{aligned} \frac{W_k - \varepsilon_k E_k}{1-\varepsilon_k} &= \sum_{i=1}^{N} F_{ki} W_i \\ -q_{net,k} &= \frac{\varepsilon_k}{1-\varepsilon_k}\left(W_k - E_k\right) \end{aligned} \tag{6}$$

Each surface in the system is seen to require the solution of two equations for two unknowns, the net emission flux W_k (via the first equation, the "W-equation") and the surface temperature T_k (influences E_k and in some cases $q_{net,k}$, via the second equation, the "T-equation").

The surface type is defined by how $q_{net,k}$ influences proceedings. A set of 3 surface types are commonly encountered in furnace analysis, and are:

- Cooled/heated element. Here, $q_{net,k}$ takes the form $U_k(T_k-T_0)$ where T_0 is the temperature of the cooling or heating medium and U_k is the total energy transfer coefficient between the surface and the medium.
- Specified flux element. Here $q_{net,k}$ is a fixed, pre-specified number. This element is useful for adiabatic surfaces ($q_{net} = 0$) or for specifying a fixed net flux such as from an arc source.
- Specified temperature element. Here T_k is a fixed, pre-specified number. This introduces some differences into the model formulation, since the T-equation is replaced by the much simpler specification, $T_k = T_{k,spec}$.

The numerical method applied to the solution of the T- and W-equations is to simply sweep through each of the surfaces in turn, calculating new W_k values (using values of T_k and W_k from the previous iteration) using the W-equation, and then do the same for the T_k values using the T-equation. Iteration over the pair of internal loops then occurs until the maximum change in estimated values between one step and the next is less than a certain small number.

Since the W-equation is linear in W_k, its approximate solution at each iteration step is found by simply solving for W_k in terms of the other W_i. For the T-equation, a new estimate of T_k is generated by applying the Newton-Raphson numerical method on T_k (since, in general, first and fourth powers of T_k are present, making analytical solution tedious), unless the surface type is constant temperature, in which case the temperature specification is simply applied.

Since the equations involved are all linear or polynomial in nature, convergence using this method is suitably rapid.

View Factors

The general radiative model as formulated above makes no assumptions as to the shape of the surface elements used to construct the system. Any such elements can be used, provided the view factors F_{ik} can be calculated.

Considering a general 3-dimensional surface in space, the best and simplest way to approximate that surface with a collection of simpler surfaces is to use flat triangular polygons. This is the higher-dimensional analogue to approximating a 2D curve with a series of straight-line segments. Just as any curve, continuous or not, can be approximated to any level of detail by using appropriately sized line segments, so any 3-dimensional surface can be similarly approximated using plane triangle segments.

The use of a triangular surface element as the base primitive for construction of 3-dimensional systems in which radiation exchange is occurring therefore allows for the greatest flexibility in terms of the geometry of said systems. It also simplifies the calculation procedure for the view factors, since only one general type of geometric arrangement need be considered.

Derivation of the general triangle-triangle view factor is performed with the aid of vector mathematics and results in a single-integral expression, which is evaluated numerically for all surface pairs in the model. Occlusion by convex parts of the 3D model is also taken into account by a shadowing algorithm.

Attenuation Model For Gas And Particles In The Freeboard

In the freeboard space between surfaces in the model, gases will generally emit and absorb radiation, and cold feed dust and fume will absorb and scatter radiation. The alteration of intensity of a beam of radiation passing through an absorbing and scattering particulate medium is shown, again in Hottel & Sarofim (1967), to be:

$$I = I_0 \exp[(-K_{a,p} - K_{s,p})L] \qquad \textbf{(7)}$$

An integral term (the source term due to scattering into the beam of radiation) has been neglected here for simplicity. The equation above may be incorporated into the view factor expression for a given pair of triangles, making the assumption that the beam length L is a constant for the pair of surfaces in question:

$$\overline{F}_{ik} = \exp[(-K_{a,p} - K_{s,p})L].F_{ik} \qquad \textbf{(8)}$$

where the overbar indicates that the contribution of scattering and absorbing material has been taken into account. The overbarred view factors are then used in place of the normal view factors in the multiple surface radiation model.

Radiation from and to gases in the freeboard space is dealt with via the calculation or measurement of gas emissivity and absorbtivity for a particular composition of gas at a particular temperature and pressure.

Dealing with radiative exchange in the presence of gas volumes is in general a considerably more complex problem than inter-surface radiation (detail scales approximately with volume versus the current treatment, which scales approximately with area). Certain simplifications can be made in cases where the entire volume may be treated as isothermal but the complexity is still great.

However, calculation of gas radiation properties using the Wide-Band model of Edwards (1981) demonstrates that, for the CO-rich atmosphere typically encountered in smelting furnace freeboards, the contribution of the gas volume to the radiative energy exchange is negligibly small (of the order of 5% or less).

Scattering and absorbtion by suspended particles may be characterised by the size range that the particles fall into. Large particles, whose characteristic dimension is very much larger than the wavelength of the incident radiation, exhibit scattering according to geometric reflections of the

incident beam. Small particles, with characteristic dimension much smaller than the incident radiation wavelength, exhibit electromagnetic scatter or refraction.

Particle effects can vary from negligible to quite significant, so direct calculation of the attenuation factors produced by fume and dust loading within the freeboard space is calculated in advance, using theory developed in Hottel & Sarofim (1967).

Data Visualisation Using VRML

Due to the difficulty inherent in describing modelling results in three dimensions as is the case here, a display format was chosen to facilitate quick and easy assimilation of a large quantity of data both geometric (the shape of the surface on which the calculations are being performed) and quantitative (data at various points on the surface such as temperatures or energy fluxes).

The Virtual Reality Modelling Language (VRML) has existed as a standard for the presentation of 3-dimensional, interactive data since the inception of the VRML 1.0 standard in 1995. VRML prescribes a format for files written in ASCII text that may be interpreted and displayed as a 3-dimensional, interactive "world" by a suitable piece of software (a VRML browser).

Various "nodes" similar in functionality to subroutines and functions in conventional programming languages allow the specification of different 3-dimensional shapes, or more abstract entities and properties such as colour, interpolation sequences or Internet hyperlinks.

An important geometry node is the IndexedFaceSet node, which allows the specification of an object constructed of or approximated by arbitrary polygonal surfaces, with the only prerequisite being that the component surfaces are flat. Each of the surfaces in the object may be assigned a unique colour and other properties, making this node particularly useful for the display of complex 3-dimensional data such as the results of the radiative exchange model.

MODEL COMPARISON AGAINST EXISTING PILOT PLANT DATA

After verification of the numerical model against simple cases for which analytical solutions exist, the effectiveness of the model in predicting the thermal behaviour of DC smelting furnace freeboard regions was evaluated. Several comparisons were performed between model predictions and actual plant data from recent large-scale pilot plant projects at Mintek.

The furnaces used at Mintek for the most part follow a generic axisymmetric design, with a cylindrical shell topped with a truncated conical roof and a flat plug at the centre. The single graphite electrode enters through the plug section. Significant differences between designs usually involve refractory choice and layout, and side-wall cooling methods.

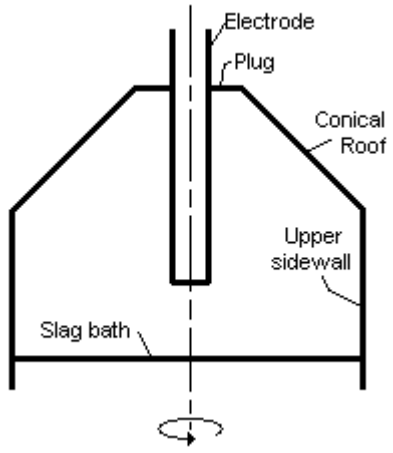

Figure 2 *- Schematic of DC arc furnace freeboard as used in radiative exchange models*

For the purposes of modelling the various cases examined, several variables and conditions were specified, along with the geometry of the system. In a furnace freeboard such as is shown above, energy is added to the freeboard by the surface of the hot molten slag bath, and is removed from the sidewall, conical roof and plug via externally cooled refractory layers. The electrode is generally not cooled in any way within the freeboard space and therefore may be assumed to be adiabatic, reradiating all of the energy impinging on it.

The net energy transfer models for the respective areas of the furnace were specified as follows:

- Slag bath – Constant temperature elements
- Sidewall – Specified heat transfer coefficient elements
- Conical roof – Specified heat transfer coefficient elements
- Plug – Specified heat transfer coefficient elements
- Electrode – Adiabatic elements

In order to evaluate the heat transfer coefficient for the elements requiring such numbers, a simplification is introduced. Assuming that the refractory layers on the sidewalls, roof and plug are thin in comparison to other dimensions of the furnace, which is generally the case, and making the approximation that conduction through the refractory is essentially one-dimensional from inside to out:

$$\frac{1}{U_n} = \frac{d_{r,n}}{k_{r,n}} + \frac{d_{s,n}}{k_{s,n}} + \frac{1}{h_{c,n}} \qquad \textbf{(9)}$$

for each surface element *n*. This gives the overall heat transfer resistance between the hot-face surface of the refractories (which is participating in the radiative exchange model) and the cooling medium, generally industrial water at 25^{O}C. d_r and k_r, and d_s and k_s are the thicknesses and thermal conductivities of refractory lining and outer steel shell respectively, and h_c is the heat transfer coefficient between the shell and the coolant. Since the cooling method used is invariably forced convection at high coolant flowrates, and the thickness of steel used in the outer shell is small, the first term dominates the above equation and allows it to be simplified even further:

$$U_n \cong \frac{k_{r,n}}{d_{r,n}} \qquad \textbf{(10)}$$

Specification of surface emissivities for the various surfaces in the freeboard region is made possible with the aid of the observation that all surfaces acquire over the course of a project a layer of variable thickness consisting of splashed or condensed process material. The only exception to this is the electrode, which is in constant motion and wears back from the arcing tip at an appreciable rate. This accretion layer is usually too thin to significantly affect the value of U_n, but it does modify the surface emissivity of surface element n to that of the process material. Although literature values for surface emissivities of typical process materials found in smelting furnaces are hard to come by, results from the calibration of pyrometer instruments used on the plant floor at Mintek suggest that $\varepsilon = 0.7$ is a very good estimate for hot or molten slag material of widely varying types. Emissivity of the electrode is taken at 0.3, a literature value for graphite.

Data from five pilot projects were used in the comparison. Cases 1 and 2 concerned Cobalt removal from slags, Cases 3 and 5 were involved with the production of Ferronickel from laterite ores, and Case 4 dealt with the production of Zinc from slags by fuming. Slag temperatures ranged from 1400 to 1700^{O}C, and refractory design varied markedly from case to case. Data was taken from a suitable series of operation periods representing a steady-state condition, for each case.

Table 1 *Results of comparison of model with experimental results*

Project	Region	Predicted kW/m^2	Measured kW/m^2
PILOT CASE 1	Upper sidewall	38.7	29.9
	Flat Roof	4.6	12.6
	Conical Roof	17.1	18.7
PILOT CASE 2	Upper sidewall	50.5	28.5
	Conical Roof	18.0	22.2
PILOT CASE 3	Upper sidewall	16.6	20.1
	Conical Roof	10.9	13.1
PILOT CASE 4	Upper sidewall	27.0	15.6
	Conical Roof	15.1	12.7
PILOT CASE 5	Upper sidewall	37.4	43.4
	Conical Roof	18.0	21.7

For the most part, the results agree fairly well with the model predictions, especially so given the state of uncertainty inherent in measurements from an industrial pilot plant and the assumptions necessary for the formulation of the model results. The correct qualitative trends are also predicted by the model, giving high energy fluxes in regions where high ones are measured, and low predictions in regions of low measured flux.

Several discrepancies do appear in the results of this comparison. It seems that the higher the energy transfer through the furnace wall, the more the model over-predicts the energy flux occurring in that region. This is particularly noticeable in the refractory regions closest to the molten slag bath, which suggests a possible explanation for the difference. Since these regions are physically closest to the molten slag (and any splashing that may result from motion of the plasma arc and solid feed material), it is highly probable that a frozen skull of slag and unreacted feed material may freeze or accrete to their surfaces, offering a significant energy transfer resistance on that portion of the wall. This would cause lower energy flux measurements than would be expected from the refractory design of the sidewall alone.

For most of the cases the discrepancy in results between model and pilot data may be explained by the presence of a nominal layer of frozen material, 2 – 7 cm thick, in the lower sidewall region of the furnace. Slag skulls have indeed been observed on the sidewalls of furnaces at Mintek, and thicknesses in the range 2 – 5 cm are common.

Qualitative Evidence To Support The Bath Radiation Mechanism

Interesting experimental evidence obtained during a recent pilot campaign at Mintek further corroborates the claim that radiation from the hot bath surface, rather than the contribution from the actual plasma arc column itself, is the most significant factor in freeboard energy losses from furnaces of this scale.

In this project, a water-cooled copper block (a “copper finger cooler”) approximately 20cm x 20cm x 50cm in dimensions was built into the upper sidewall brickwork, just below the junction of the conical roof and the cylindrical crucible. The block was built into the wall such that its front 20cm x 20cm face was very close to, if not directly exposed to, the freeboard volume, to act as an energy flux sensor.

Since copper conducts thermal energy far better and faster than the refractories, an examination of the transients that occur in the measurement of energy losses from this block when for some reason the power in the furnace is shut down for a significant period of time can give insight as to the mechanism of radiation energy loss occurring. If the freeboard losses are as a result of direct radiation from the plasma arc, one would expect the copper finger losses to drop off very rapidly, since the net energy flux impinging on the face of the cooler will have made an abrupt step change down to zero. If, on the other hand, the losses are due to radiation from the molten bath, one would expect the copper finger losses to drop off far more slowly, since the energy source driving the freeboard energy losses in this case is still present, even though the actual furnace power is off.

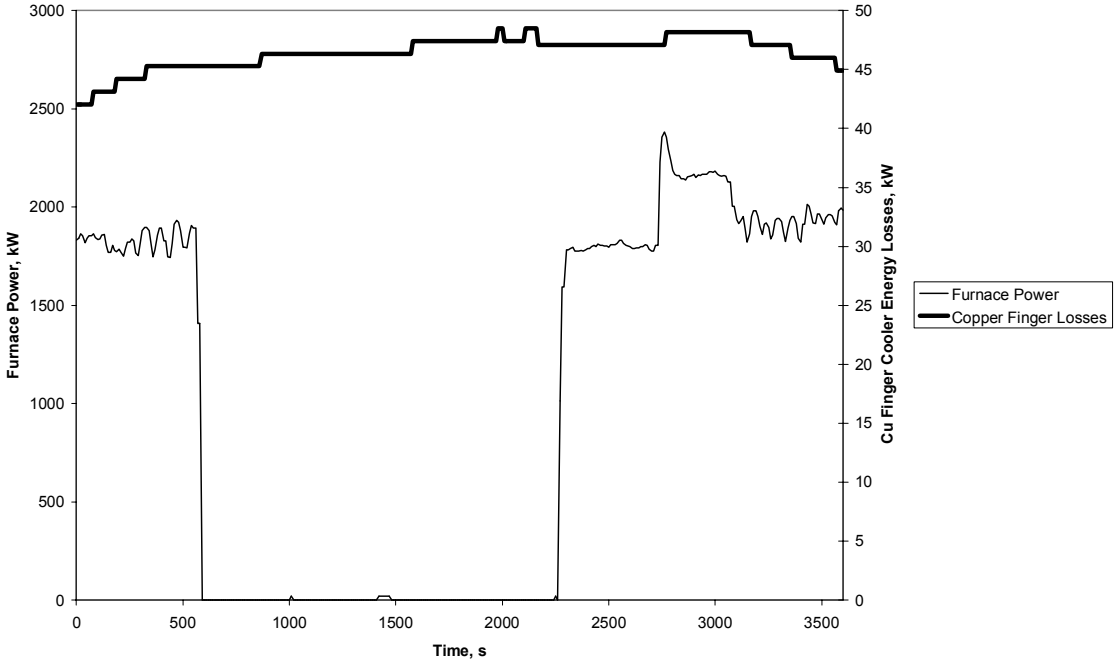

Figure 3 - *Copper finger cooler transient in response to power outage*

As can be seen clearly in figure 3, at this point in the project, after having run stable for several hours, the furnace power is shut down for around twenty-five minutes (at 600s on the graph). The transient trend of the copper cooler energy loss exhibits no sudden drop at all over this entire period, continuing in fact to *rise*, presumably as the dust and fume clear out of the freeboard space in the absence of feed and arc, and enable the cooler face to more clearly see the bath surface.

It would therefore appear that freeboard energy losses, at least on typical pilot-scale furnaces, are dominated by radiation from the hot, molten bath surface.

EFFECT OF VARIABLES ON THE MODEL

The fully developed surface re-radiation model was used in a detailed examination of the effects of DC-arc furnace design and process variables on the thermal behaviour. The approach consisted of comparing the behaviour to a common "base case" while varying each examined variable in isolation. This base case furnace design follows closely the design of the large-scale 5.6MVA pilot plant furnaces used at Mintek, with a furnace vessel approximately 2m in diameter and 2.5m high. Some examples, and discussion, follows.

Effect of scale

The effect of scaling up the dimensions of the furnace freeboard geometry (note that refractory design remains the same as the freeboard is scaled up) is negligibly small indeed. An order-of-magnitude variation in furnace size, from 1m diameter to 12m, produces differences in surface temperatures and energy fluxes in all regions that are small enough to be attributed to numerical inaccuracies. This effect is illustrated in figure 4.

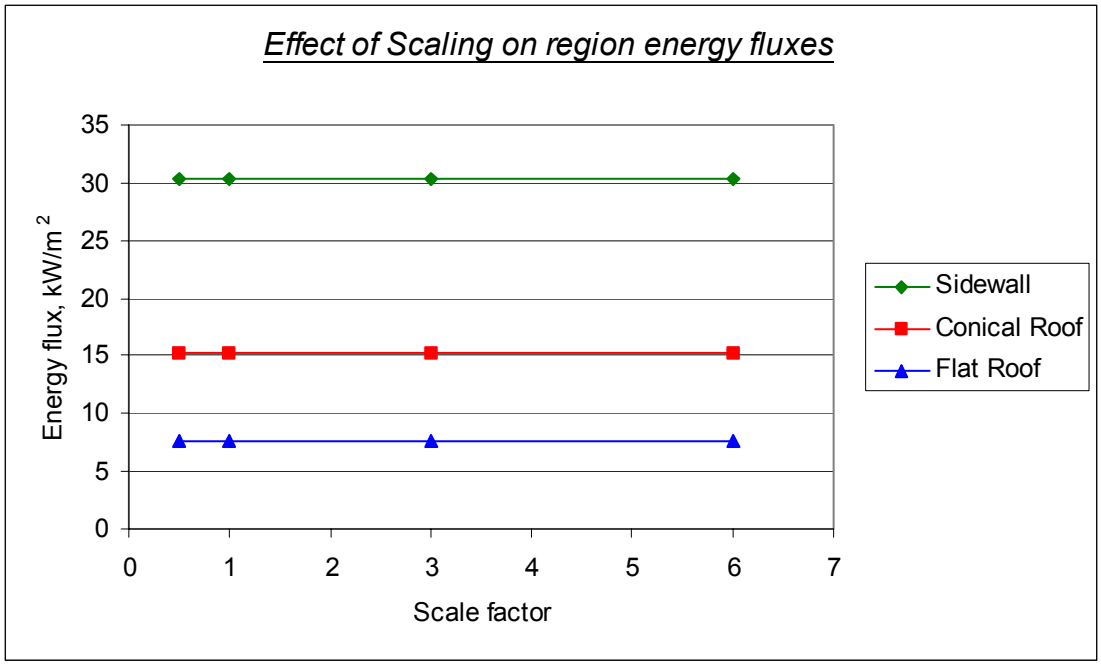

Figure 4 *– Graph showing effect of changing the furnace scale*

Effect of attenuation factor

The effect of attenuation of radiative energy in the freeboard space by an interposing medium can be pronounced. With the caveat that this is a very simplistic model in terms of its ability to deal with absorption, emission and scattering by dust and fume in the gas space, several interesting effects appear as the attenuation factor increases from zero in both the industrial and pilot-scale results.

The bulk effect of an increase in attenuation factor is to lower the energy flux received by all freeboard surfaces, as the attenuating medium intercepts more and more of the thermal radiation in the freeboard space. A more subtle effect is an increase in the spread of surface temperatures inside the furnace gas space, with the ranges growing to span an order of magnitude or more in some cases. The most noticeable area exhibiting this behaviour is the upper sidewall. The presence of an attenuating medium is thus a double-edged sword to some degree, offering decreased net energy losses from the furnace freeboard while increasing the chance of fracture and spalling due to very large thermal gradients in contiguous refractory zones.

Attenuation in the freeboard space can also produce a scale-dependent effect that may cloud the issue of accurate scale-up calculations. It is seen from figure 5 that while the re-radiant energy losses from the pilot-scale case (a 2m diameter furnace) are still very significant at a factor of 0.5 – 1.0, a similar factor in the larger industrial-scale case (a 12m diameter furnace) would lead to almost complete attenuation of all re-radiant energy, and very good shielding of the freeboard surfaces by the attenuating medium. A direct measurement (by sampling or otherwise) of the dust and fume loading inside the freeboard space on the pilot scale is thus considered to be of considerable value when the time comes to scale to an industrial design.

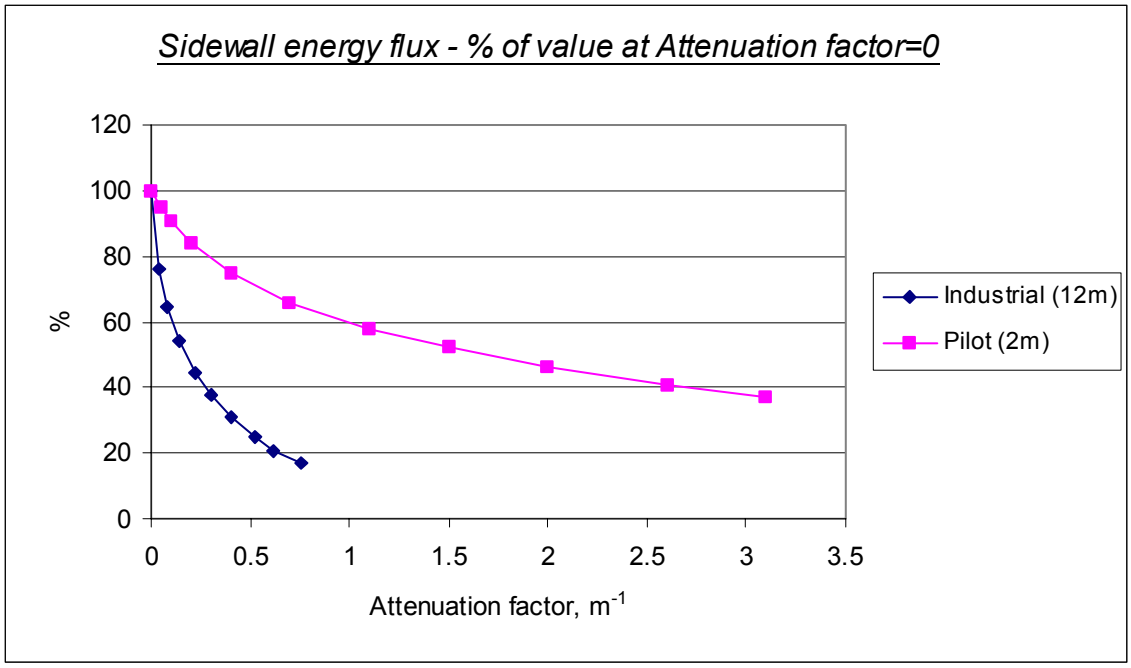

Figure 5 - *Graph showing effect of furnace size on the attenuation of radiation*

Effect of changing U-values
Altering the heat transfer coefficient value on any of the cooled surfaces in the freeboard model produces a pronounced effect on both the temperature and energy flux distribution within the furnace. The surface whose U-value is changed experiences the most dramatic change, generally decreasing in temperature and increasing in energy flux as U is increased. The effect on the remaining surfaces in the model is generally to decrease marginally in both energy flux and temperature.

Using a more conductive wall design on the upper sidewall or roof regions would allow all regions in the furnace freeboard to operate cooler, at the expense of greater total energy losses and higher sustained energy fluxes.

Effect of furnace diameter
Reducing the furnace diameter, with all other dimensions fixed, results in a drop in both surface temperatures and energy fluxes in all regions, with the decrease accelerating as the diameter decreases. The results would seem to suggest that this effect becomes very significant at diameters smaller than 1.5m for this particular case.

Effect of sidewall height
Increasing the height of the furnace sidewall section exposed to the freeboard space is seen to decrease the temperatures and energy fluxes in all regions. The effect is small, however, with net energy fluxes through the freeboard regions decreasing only 5 – 10% at most. Since the net surface area increases linearly with increasing sidewall height, the net energy loss will also increase.

Effect of roof angle
The roof angle (varied by varying the height of the roof plug above the surface of the slag bath, and measured from the horizontal) produces several interesting effects. The gross effect is a decrease in surface temperatures and energy fluxes in all regions as the roof angle increases, although this may also be attributed to the increase in total roof surface area incurred by the method of altering the angle.

A secondary effect concerns the spread of temperatures on the upper sidewall and roof. As the angle increases from zero, the spread of temperatures in both these regions appears to go through a minimum around 40^{o}, with the maximum and minimum temperatures getting fairly close to the average. Identifying this minimum would prove useful in terms of minimising the temperature variance across a contiguous region of refractory (such as the roof or sidewall sections) in order to minimise the thermal stresses in these areas.

Effect of emissivity
The grey-body surface emissivity of the refractory regions of the furnace has a large impact on the thermal behaviour of the furnace freeboard. As the emissivity drops, the surface temperatures and net energy fluxes in all regions drop with it, accelerating as the emissivity approaches zero.

The emissivity of the various surfaces within the furnace freeboard space is difficult to enforce as a design variable. It will rather tend to be a function of the type of refractory used to line that portion of the vessel (which is most likely to be chosen for properties other than its emissivity), as well as a function of the process itself. After prolonged operation one might reasonably expect to see much of the furnace interior coated with at least a thin layer of process material, potentially altering its emissivity considerably.

Effect of slag surface temperature
Unsurprisingly, the temperature of the surface of the slag bath in the furnace has an enormous impact on the thermal behaviour, since this surface is ultimately the source of all energy in the freeboard re-radiation model. As the slag temperature increases, the surface temperatures and the energy fluxes in all regions follow it almost linearly.

CONCLUSIONS

The development and use of a general model of thermal radiation interchange from surfaces has been successful to some degree in explaining the energy distribution and thermal behaviour of the freeboard region in the DC plasma arc furnace. Comparison to data from the 1-2MW scale indicates that radiation from the hot, open bath is the principal source of energy loss from this region, not the plasma arc column. Changing various design and process variables in the model was seen to produce interesting and occasionally unexpected results in the thermal behaviour of the freeboard space.

REFERENCES

Bowman, B., 1990, Effects on furnace arcs of submerging by slag, Ironmaking and Steelmaking, No. 2.
Bowman, B., 1994, Properties of arcs in DC furnaces, In: Electric Furnace Conference Proceedings.
Brent, A., 1989, A computational analysis of heat transfer and fluid flow in plasma melting furnaces, PhD Thesis, University of Minnesota.
Deneys, A.C. & Robertson, D.G.C., 1998, Fluid Flow Phenomena in a Laboratory Scale DC Arc Furnace for Slag Cleaning, Iron and Steel Society Technical Paper.
Edwards, D.K., 1981, Radiation Heat Transfer Notes, Hemisphere.
Gu, L., Jensen, R., & Bakken, J.A., 1993, Metal vapour infiltration in argon arcs used for heating liquid metal, In: Electric Furnace Conference Proceedings.
Holt, N.J. & Bakken, J.A., 1993, Transferred Argon Arc Reactor With Emphasis On Radiation Heat transfer, In: Electric Furnace Conference Proceedings.
Hottel, H.C. & Sarofim, A.F., 1967, Radiative Transfer, McGraw-Hill.
Sawicki, A. & Krouchinin, A.M., 1998, Modelling of the cylindrical part of the effective arc in steelmaking AC arc furnaces, Elektrowarme International, December.
Shamsi, M.R.R.I., 1994, Turbulent fluid flow modeling to predict the heat transfer in the plasma furnace, PhD thesis, Indian Institute of Technology.
Szekely, J., McKelliget, J. & Choudhary, M., 1983, Heat-transfer fluid flow and bath circulation in electric-arc furnaces and dc plasma furnaces, Ironmaking and Steelmaking, No. 4.
Ushio, M., Szekely, J., & Chang, C.W., 1981, Mathematical modelling of flow field and heat transfer in high-current arc discharge, Ironmaking and Steelmaking, No. 6.